Vibration Control By A TMD Using A Rotating Inertial Mass

Tetsuya HANZAWA & Kazuhiko ISODA
Shimizu Corporation, Japan

SUMMARY
A TMD system using a rotating inertial mass damper is proposed to reduce vertical vibration of structural beams and floor slabs subject to walking excitation and earthquake motions. The newly developed TMD is comprised of a ball screw mechanism including flywheels and springs. This system has proven to have significant mass effects because of the ball screw mechanism, even with a small mass of the flywheel. The authors conducted vibration tests to validate the effects of the TMD using a rotating inertial mass, and compared the test results with simulation analyses.

Keywords: Rotating inertial mass Vertical vibration control Tuned mass damper

1. INTRODUCTION

Floor vibrations subject to walking excitation may even make residents uncomfortable in a structure using beams and floors placed in wide spans. Vertical seismic vibrations may also be one of the causes of goods jumping on the floor and falling or tumbling of fixtures to damage. As a countermeasure against such occurrences, viscoelasticity dampers and TMD (Tuned Mass Damper) may be effective to control vertical vibrations.

TMD is, as well known, to attune natural frequencies of adding vibration systems to natural frequencies of a main system, which is to absorb vibrational energy of the main system and reduce its responses. With this system, the higher the mass ratio of the damper (ratio of the mass of the damper and main system), the larger the damping effects. However, if the mass of the damper is excessive, it could be an unwanted load to the main structural members.

This paper proposes a new TMD using large inertial effects given by a ball screw mechanism.

2. CONFIGURATION OF ROTATING INERTIAL MASS DAMPER

Figure 2.1. shows a mass device to be used for the TMD system referred to in this paper, as a “rotating inertia mass damper”. This device is comprised of a ball screw and flywheel. This system allows a linear motion of the ball screw of the main system vibrating, which is followed by a circular motion of the flywheel and ball nuts. A displacement to rotate a ball nut in a cycle is called Lead L_d. A work E to generate a displacement x by placing a force to push the ball screw F is shown as Formula (2.1). Formula (2.2) is to calculate a work W to lead rotation θ at a moment M of the rotating ball nut and flywheel. Both formulas are consistent if no friction is assumed. The relationship of the lead and displacement, Formula (2.3), will be the basis of Formula (2.4), which shows that F is proportional to the acceleration of the linear direction. Coefficient Ψ is equivalent to the inertial mass. Assuming I_θ as a rotating inertia moment of the disk in diameter D and mass m, Ψ shall be described as Formula (2.5) so that the value shall be some hundreds to thousands times of the actual mass m.

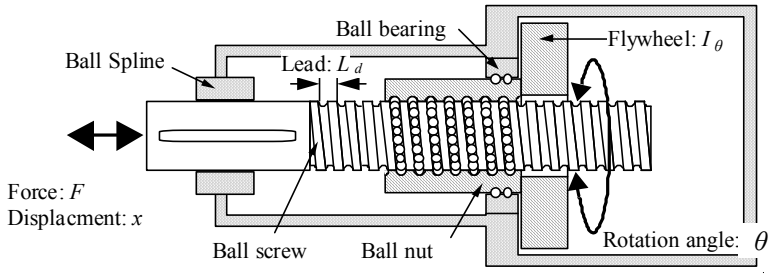

Figure 2.1. Ball Screw Mechanism

$$E = Fx \tag{2.1}$$

$$W = M\theta = I_\theta \ddot{\theta}\theta \tag{2.2}$$

$$\theta = \frac{2\pi}{L_d}x \tag{2.3}$$

$$F = \left(\frac{2\pi}{L_d}\right)^2 I_\theta \ddot{x} = \Psi \ddot{x} \tag{2.4}$$

$$\Psi = \frac{1}{2}\left(\frac{\pi D}{L_d}\right)^2 m \tag{2.5}$$

3. DAMPING SYSTEM USING ROTATING INERTIAL MASS DAMPER

Figure 3.1. shows a typical damping system using the device in the previous section. The damping system shown in Figure 3.1. has plate springs and rotating mass dampers (hereinafter, inertial mass damper) under the beams, which is a main structure. The plate springs and inertial mass dampers are connected and supported by a member. Its dynamics model is as shown in Figure 3.2. Formula (3.1) is the equation of vibration, not considering damping of the main system. Assuming stationary response, the acceleration amplification factor is calculated as Formula (3.2). For the parameter μ, the optimum η and β_d of Formula (3.3) are applied to Formula (3.2) as illustrated in Figure 3.3. It shows that the higher damping the larger mass ratio, in the same manner as the TMD. However, its design is different from a conventional TMD, as which is effective enough only by placing the device on the floor, since this system needs a structure to install the damper.

$$\begin{bmatrix} m & 0 \\ 0 & \Psi \end{bmatrix}\begin{Bmatrix} \ddot{X} \\ \ddot{X}_d \end{Bmatrix} + \begin{bmatrix} 0 & 0 \\ 0 & C_d \end{bmatrix}\begin{Bmatrix} \dot{X} \\ \dot{X}_d \end{Bmatrix} + \begin{bmatrix} 0 & 0 \\ 0 & C_d \end{bmatrix}\begin{Bmatrix} X \\ X_d \end{Bmatrix} = \begin{Bmatrix} f \\ 0 \end{Bmatrix} \tag{3.1}$$

$$\frac{\ddot{X}}{a} = -\frac{\mu\xi^2\left(\eta^2 - \xi^2\right) + i\beta_d\mu\xi^3\eta}{-\mu\left((\mu+1)\xi^2\eta^2 - \eta^2 - \xi^4 + \xi^2\right) + i\beta_d\mu\xi\eta\left(\mu\eta^2 - \xi^2 + 1\right)} \tag{3.2}$$

$$\eta = \frac{1-\sqrt{1-4\mu}}{2\mu}, \beta_d = \frac{\sqrt{3\left(1-\sqrt{1-4\mu}\right)}}{2} \tag{3.3}$$

Here, $\mu=\Psi/m$: mass ratio of damper, a=f/m: external force standardized with a mass of the main system, $\xi=\omega/\omega_1$: stimulus circular frequency ratio, ω: stimulus circular frequency, $\omega_f^2=k/m$: natural circular frequency of the main system, $\eta=\omega_d/\omega_f$: natural circular frequency ratio of a damper, $\omega_d^2=k_d/\Psi$: natural circular frequency of a damper, $\beta_d=2h_d$: damping constant (multiple number), and $h_d=c_d/(2\Psi\omega_d)$: damping constant.

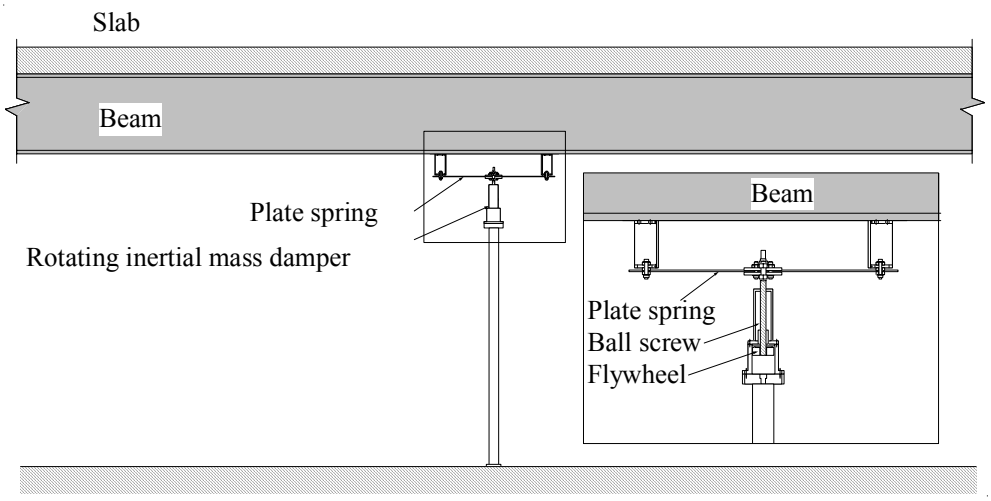

Figure 3.1. Damping System using Rotating Inertial Mass Damper

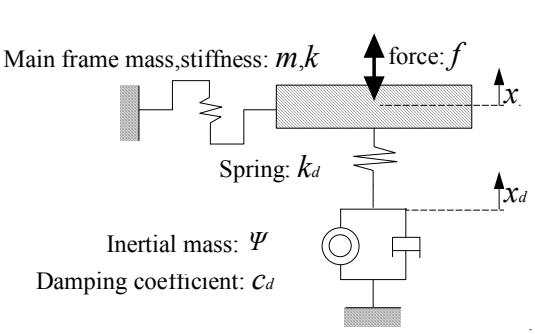

Figure 3.2. Damping System Model

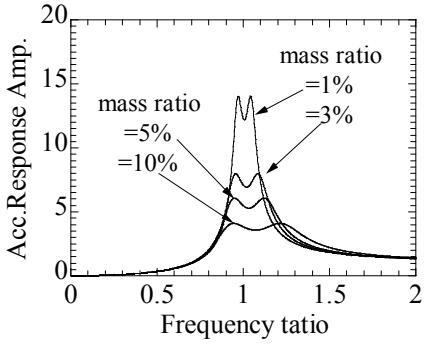

Figure 3.3. Acceleration Response Amplification

It is assumed that there shall be another damping system using an inertial mass damper, other than that of Figure 3.1. Figure 3.4. shows an example.

Figure 3.4. (a) shows a structure with tension members placed from both sides of the beam within the length of the beam. An inertial mass damper is placed in the center of the tension member. The inertial mass damper is connected to the beams. In order to apply a tensile force to the tension members, these members are pulled from a certain points under the beam, with a spring placed in between the members. The point to place the spring for keeping the tensile force of the tension members is different from the system in Figure 3.1. With this method, there should be no supports for the inertia mass damper, so that the degree of freedom is improved in the area under the beams. This is advantageous compared to the method shown in Figure 3.4. (a).

Figure 3.4. (b) shows a system to have the truss beam to support the inertial mass damper. The stiffness of springs in series, which is comprised of the truss beam and the adjustment plate spring, must be consistent with the stiffness required for attuning with the damper.

As the structure shown in Figure 3.4. (c) has the support column for the inertial mass damper is located in the lower floor, the mass is large as equivalent to that of the upper floor for the structure, which is different from the design shown in Figure 3.1. However, there is no effect if the natural frequencies in the lower and upper floor are close in value.

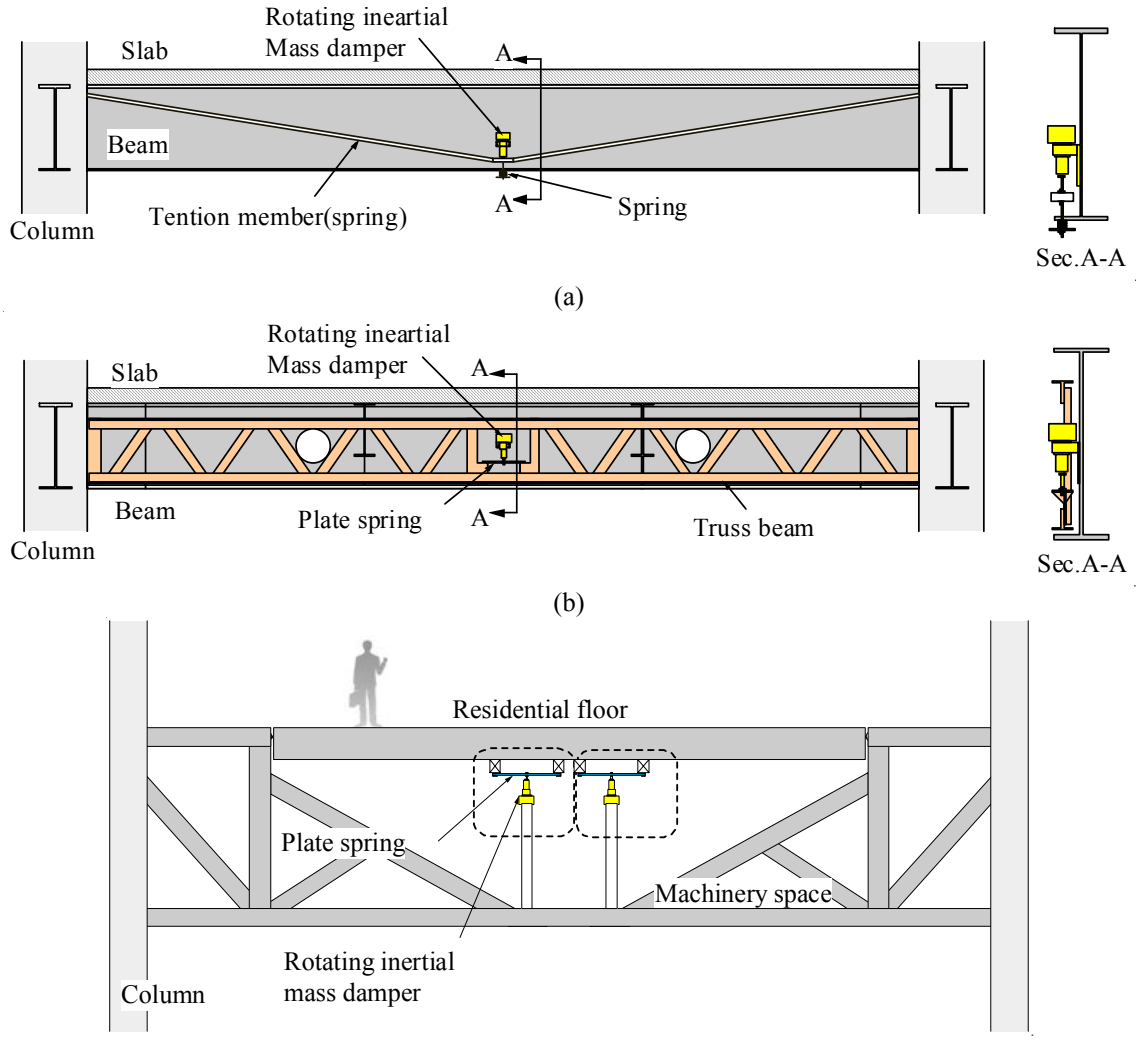

Figure 3.4. Various Features of Damping Systems

4. TEST AND SIMULATION

4.1. Outline of Damping System Behavior in case of Earthquake

A vibration test is conducted for Figure 3.4. (c) to validate damping effects against seismic vibration. Figure 4.1 shows the specimens. The specimen is a two-story structure placed on a shaking table. As stated below, the natural frequencies of the first and second floors are approximately 8.9Hz and 4.5Hz respectively. The specimen is designed to have a span for 30% of the actual building supposed to be. Natural frequencies of each floor are almost equivalent to the building in assumption. An inertial mass damper (lead size 10mm) and a coil spring are installed in series between the two floors.

Excitation waves include White noise, constant amplitude sweep waves in the range from 2 to 6Hz (10cm/sec^2) and three types of seismic waves. The seismic waves include a strong motion record and simulated earthquake motion. Table 4.1. and Figure 4.2. show the list of seismic waves and the acceleration response spectrum (damping 1%) respectively. As the span is in length for 30% of the actual design of a building assumed, the input level is also specified as 30% for the design earthquake motion.

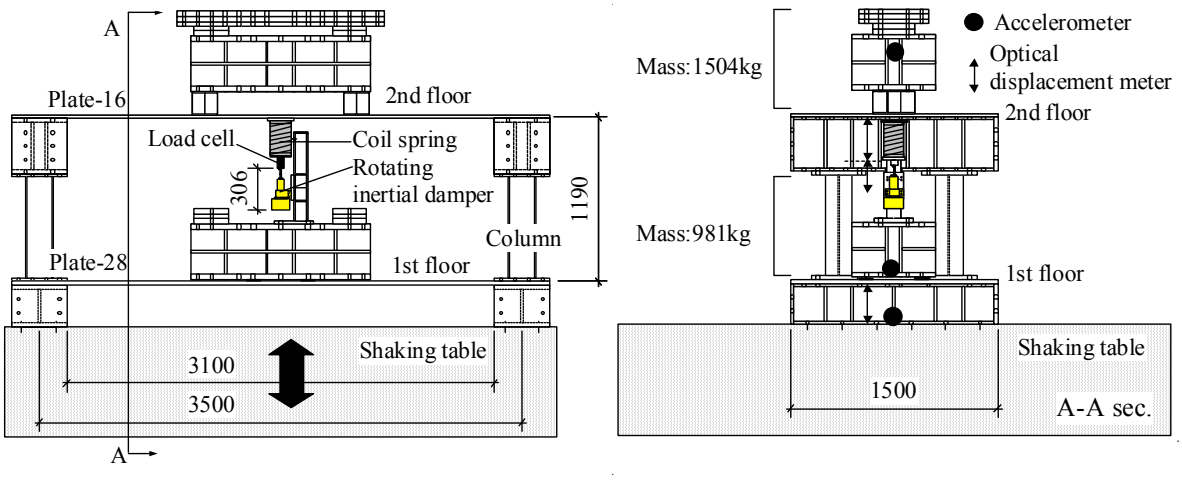

Figure 4.1. Specimen (unit: mm)

Photo 4.1. Specimen

Table 4.1. Seismic Wave List

Wave	Direction	Maximum Acceleration	Duration	Time interval
El centro 30%	UD	92.3 cm/sec^2	60 sec	0.01 sec
TAFT 30%	UD	88.7 cm/sec^2	60 sec	0.01 sec
Art Wave 30%	UD	61.1 cm/sec^2	60 sec	0.01sec

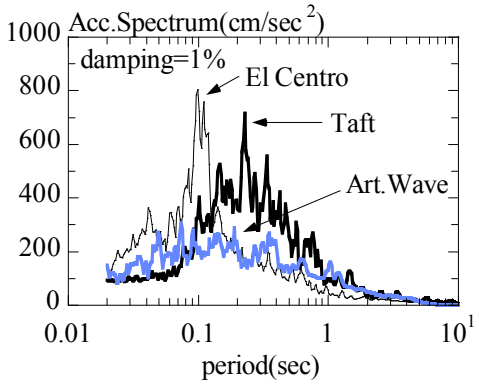

Figure 4.2. Response Spectrum of Seismic Wave

4.2. Test Results

Figure 4.3. shows transfer functions of the shaking table, first floor and second floors for White noise excitation. With no inertial mass damper, natural frequencies of the first and second floors are 4.5Hz

and 8.9Hz respectively. If there is an inertial mass damper, the peak for the second floor is at a lower level.

The response acceleration, against the sweep excitation of 2-6Hz, monitored for the second floor, is as shown in Figure 4.4. It shows sympathetic vibration at around 190 seconds for the structure without a damper. No sympathetic vibration was monitored for the structure with a damper.

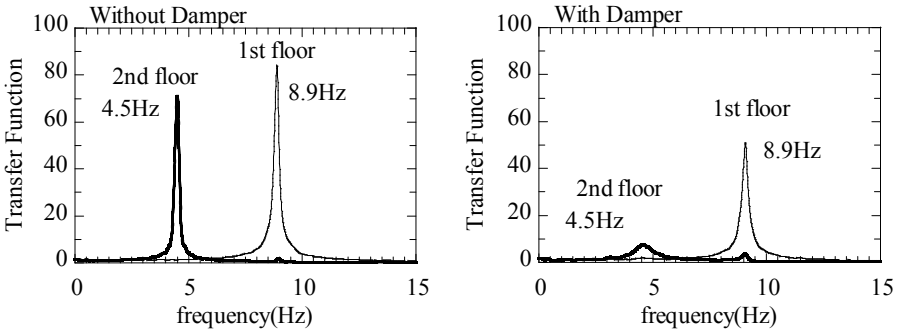

Figure 4.3. Transfer Function

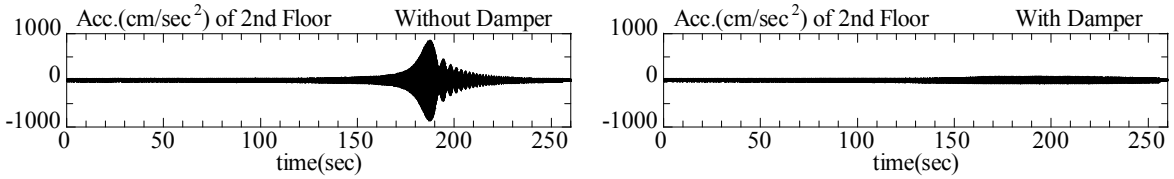

Figure 4.4. Acceleration Response Wave for the Second Floor with Sweep Excitation

Figure 4.5. shows some examples of the load-deformation relationship of the inertial mass damper when applying sweep excitation. Formula (2.4) is substituted by Formula (4.1) for sine waves. It shows that the load and deformation of the inertial mass damper becomes a negative slope.

$$F = \left(\frac{2\pi}{L_d}\right)^2 I_\theta \ddot{x} = \Psi \ddot{x} = -\omega^2 \Psi x \tag{4.1}$$

As the load-deformation relationship shown in Figure 4.5. has a negative slope, the test also revealed that the inertial mass damper has mass effects, as well as energy absorption to occur. The inertial mass is calculated from the slope as Figure 4.6., which is approximately 118kg. The mass of an actual inertial mass damper and flywheel are 9kg and approximately 200g respectively

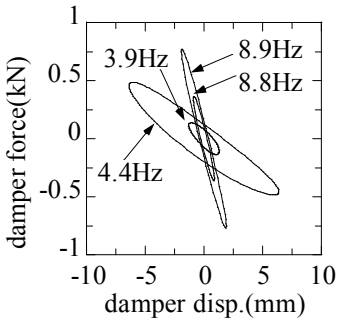

Figure 4.5. Load-deformation Relationships of Damper

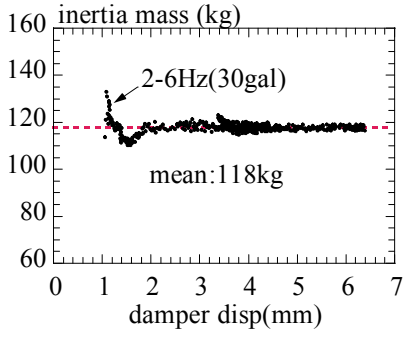

Figure 4.6. Inertial Mass of Damper

Figure 4.7. shows the acceleration response wave at the second floor related to seismic waves. Cosine filters of 1-10Hz are applied to the acceleration data in order to eliminate impacts of high frequencies. The comparison of the peak accelerations of the second floor is as shown in Table 4.2. Although it depends of types of seismic waves, the response acceleration due to earthquake is reduced by about 30-70% with the damper.

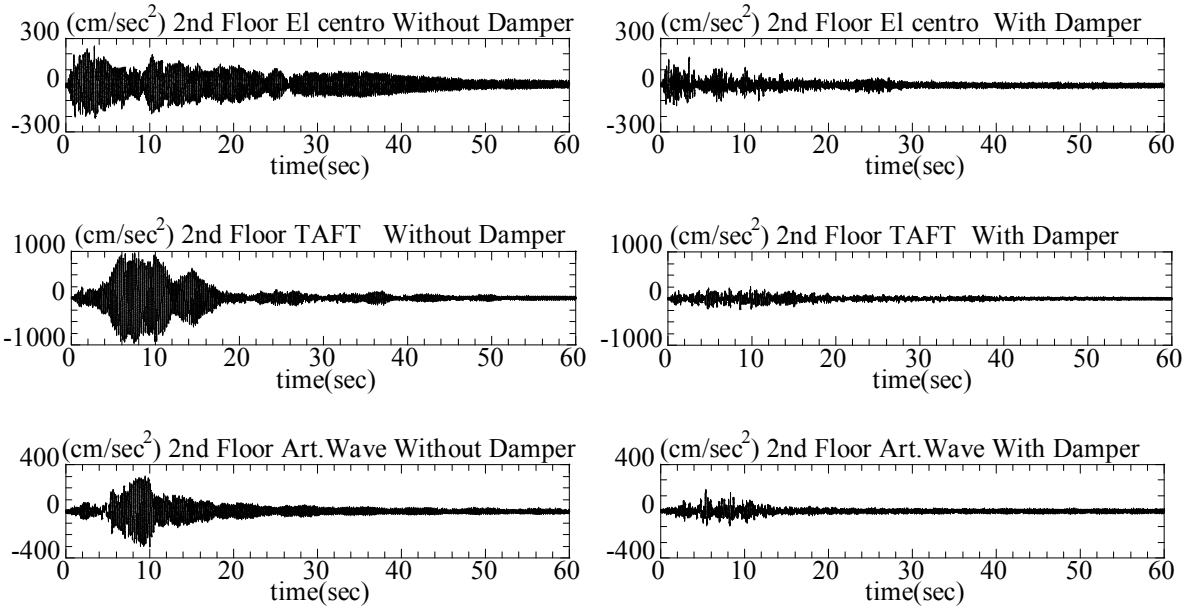

Figure 4.7. Acceleration Response Wave due to Seismic Wave for the Second Floor

Table 4.2. Test Results for Reduction of Maximum Acceleration

	Without Damper	With Damper	
	Maximum Acceleration (2nd Floor)	Maximum Acceleration (2nd Floor)	Ratio
El centro 30%	247 cm/sec^2	170 cm/sec^2	0.69
TAFT 30%	958 cm/sec^2	240 cm/sec^2	0.25
Art Wave 30%	295 cm/sec^2	171 cm/sec^2	0.58

As above, the following summarizes the knowledge led by the tests.

1) A damping system proposed in this paper shows effects decreasing, compared to the case without inertial mass dampers, as a result of the excitation test using transfer functions with White Noise, sweep excitation and seismic waves.
2) Inertial mass dampers have mass effects for about 600 times of that with a flywheel.
3) Inertial mass dampers are proven to have energy absorbing capabilities.

4.3. Simulation

This section delineates a simulation analysis of the test results.

Figure 4.8. shows the analytical model. As there are bolts placed between the weight of the specimen and the floor plate, a rotating spring is installed to specify a spring constant to cope with natural frequencies given by a transfer function. Damping constants of the structure is designed to reproduce the peak acceleration of the test results, with 0.25% and 0.3% of Rayleigh damping for the primary and secondary sides respectively. The spring constants are 1.36×10^5N/m for a tension side and 1.14×10^5N/m for a compression side, as a result of the test assuming an earthquake. The spring constants are different from the compression and tension sides due to the coil spring.

As stated earlier, the inertial mass is designed as 118kg for the inertial mass damper. In terms of damping, viscous damping is calculated to quantify as the formula below according to the test results

of three types of seismic responses. Here, P_v: viscous damping , F: damper force, Ψ: inertial mass, and X_d: damper displacement are applied. Figure 4.10. shows viscous damping and viscous damping coefficients.

$$P_v = F - \Psi \ddot{X}_d \tag{4.2}$$

Table 4.3. and Figure 4.9. show the analytical results of an eigen value analysis for a structure without dampers. As the equivalent mass of the second floor is 1068kg, its mass ratio is considered to be μ=11%.

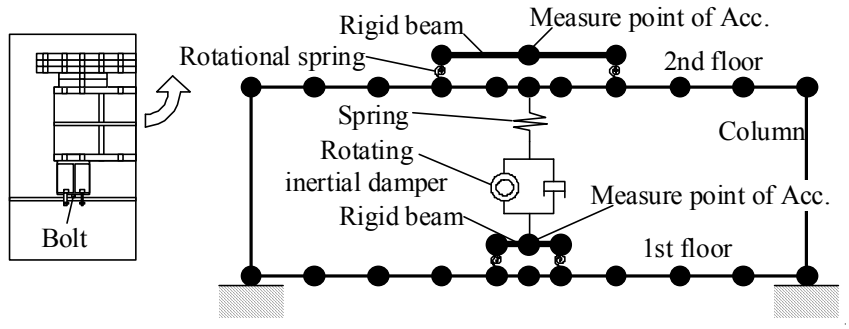

Figure 4.8. Analytical Model

Table 4.3. Eigen Value Analytical Results

Order	Natural Frequencies	Participation Factor	Effective Mass	Equivalent Mass
1	4.47 Hz	1.34	1922 kg	1068 kg
2	8.89 Hz	1.10	1661 kg	1377 kg

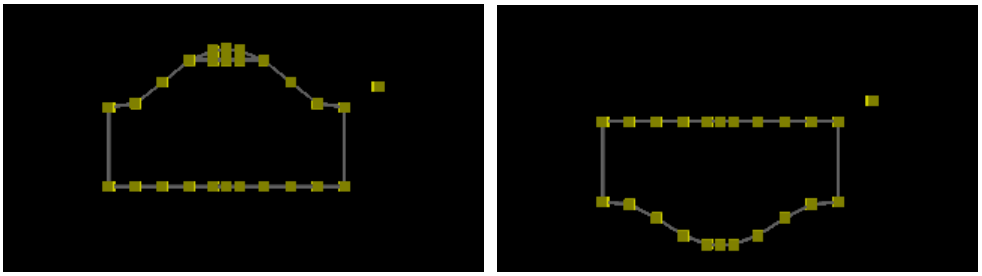

Primary Mode Secondary Mode

Figure 4.9. Modes for Structures without Damper

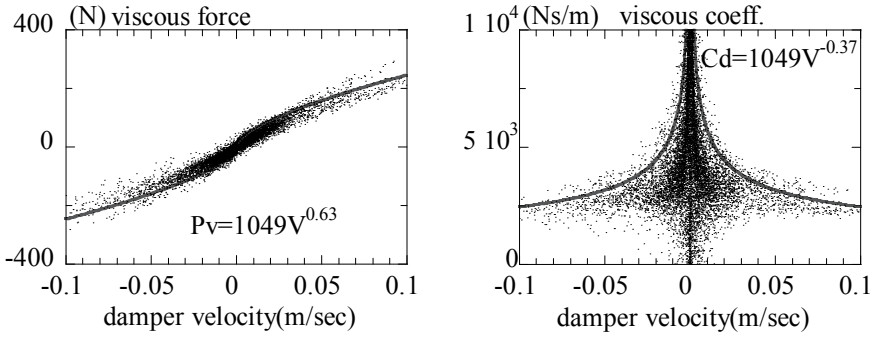

Figure 4.10. Damping Force Model

Figure 4.11. shows the response acceleration wave for the second floor when the artificial earthquake wave is input for the structure without damper. The comparison of the peak accelerations of the

second floor is as shown in Table 4.4. The response acceleration from the analytical model is consistent with the test results.

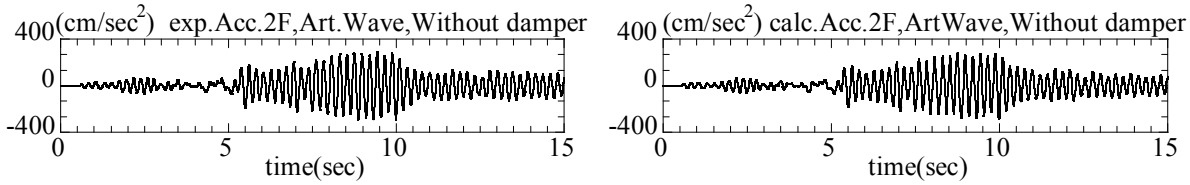

Figure 4.11. Comparison of Seismic Response Wave for the Structure without Damper (case of Art.Wave)

Table 4.4. Comparison of the Peak Acceleration due to Earthquake for the Structure without Damper

	Without Damper		
	experiment	calculation	
	Maximum Acceleration (2nd Floor)	Maximum Acceleration (2nd Floor)	Ratio
El centro 30%	247 cm/sec^2	230 cm/sec^2	0.93
TAFT 30%	958 cm/sec^2	985 cm/sec^2	1.03
Art Wave 30%	295 cm/sec^2	284 cm/sec^2	0.96

Figure 4.12. shows the response acceleration wave monitored at the second floor for the structure with damper, as the artificial earthquake wave is input. Table 4.5. shows a comparison of the peak accelerations of the second floor. Figure 4.13. and Figure 4.14 show the load-deformation relationship of the dampers for test and calculation relatively. The test results are reasonable for the response acceleration of the analytical model and the load-deformation relationship of the damper.

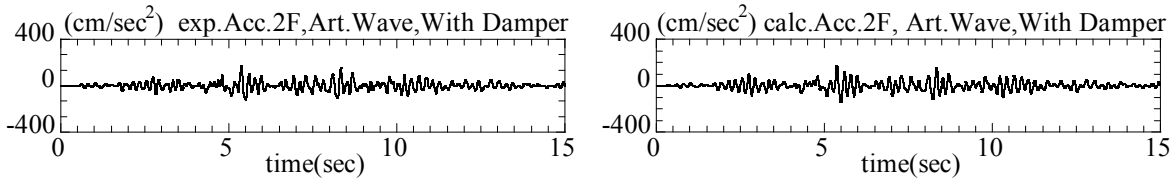

Test Results Analytical Results

Figure 4.12. Comparison of Seismic Response Wave of the Structure with Damper(case of Art.Wave)

Table 4.5. Comparison of the Peak Accelerations due to Earthquake for the Structure with Damper

	With Damper		
	experiment	calculation	
	Maximum Acceleration (2nd Floor)	Maximum Acceleration (2nd Floor)	Ratio
El centro 30%	170 cm/sec^2	162 cm/sec^2	0.95
TAFT 30%	240 cm/sec^2	241 cm/sec^2	1.00
Art Wave 30%	171 cm/sec^2	169 cm/sec^2	0.99

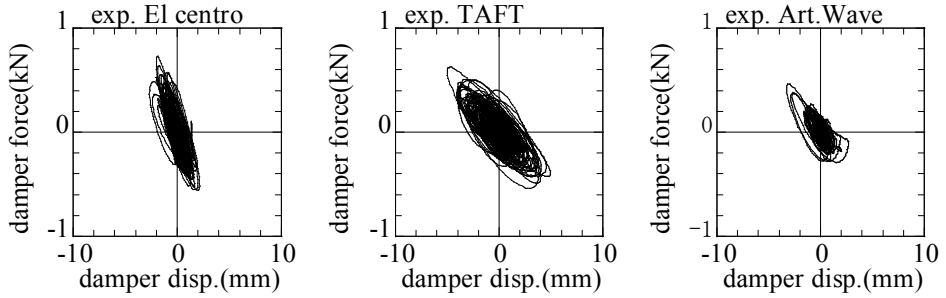

Figure 4.13. Load-deformation Relationships of Inertial Mass Damper and Spring (Test)

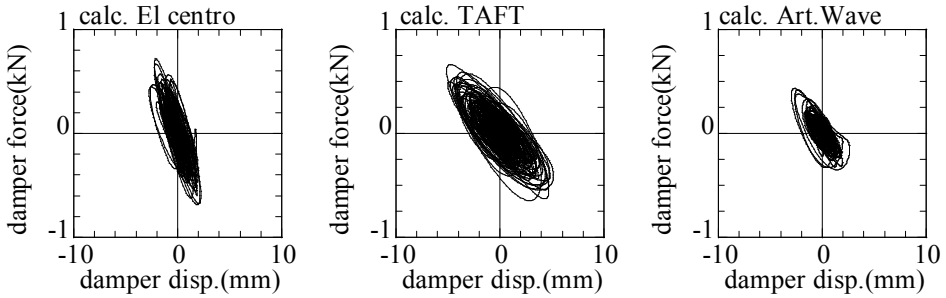

Figure 4.14. Load-deformation Relationships of Inertial Mass Damper and Spring (Analysis)

5. CONCLUSION

This paper proposes a damping system with rotating inertial mass dampers to reduce vertical vibration to occur with beams and floors of a structure. The rotating inertial mass damper has a significant inertial mass effect, in spite of its small mass. The proposed damping system, one of the types of TMD mechanisms, has mass effects to synchronize with movements of the main circuit. Therefore, this system achieves a large mass ratio by using small and lightweight devices. Vibration tests are also conducted for the damping system of a double-slab, which also shows reasonable damping effects. The simulation analysis also indicates reasonable results from both test and analysis.

ACKNOWLEDGEMENT

We would like to thank Mr. Mikio Yanagisawa and Mr. Hidenobu Kadowaki, structural design department, Shimizu Corporation, for their useful suggestions..

REFERENCES

J.P.Den Hartog (1956). Mechanical Vibrations, 4th ed., McGraw-Hill Book Compary, Inc.

Tetsuya, H. and Kazuhiko, I.(2009). Experimental Study on Vertical Vibration Control by A TMD Uisng A Rotating Inertia Mass. *Journal of Structural and Construction Engineering*, **74:640**, 1047-1054.

Kenji, S.,Shigeki,N.,Hidenori, K. and Norio, I.(2008). Vibration Tests of 1-Story Response Control System Using Inertial Mass And Optimaized Softy Spring And Viscous Element. *Journal of Structural Engineering*, **Vol.54B**, 623-634.

Tetsuya, H. and Kazuhiko, I.(2009). Vibration Control by A TMD Using A Rotating Inertia Mass. , **15:31**, 691-696.

Tetsuya, H. and Kazuhiko, I.(2010). Floor Vibration Control by A TMD Using A Rotating Inertia Mass. *Journal of Structural Engineering*, **Vol.56B**, 213-220.